

M3H: Multimodal Multitask Machine Learning for Healthcare

Dimitris Bertsimas¹, Yu Ma²

¹Sloan School of Management, Massachusetts Institute of Technology, USA

dbertsim@mit.edu

²Operations Research Center, Massachusetts Institute of Technology, USA

midsumer@mit.edu

Abstract

Recent breakthroughs in artificial intelligence (AI) are poised to fundamentally enhance our existing study and understanding of healthcare. Specifically, the development of an integrated many-to-many framework that leverages multiple data modality inputs for the analytical modeling of multiple medical tasks, is critical for a unified understanding of modern medicine. In this work, we introduce M3H, an explainable Multimodal Multitask Machine Learning for Healthcare framework that consolidates learning from diverse multimodal inputs across a broad spectrum of medical task categories and machine learning problem classes. The modular design of the framework ensures its generalizable data processing, task definition, and rapid model prototyping, applicable to both clinical and operational healthcare settings. We evaluate the M3H framework by validating models trained from four modalities (tabular, time-series, language, and vision) on 41 medical tasks across 4 machine learning problem classes. Our results demonstrate that M3H consistently produces multitask models that outperform canonical single-task models (by 1.1-37.2%) across 37 disease diagnoses from 16 medical departments, three hospital operation forecast, and one patient phenotyping tasks: spanning machine learning problem classes of supervised binary classification, multiclass classification, regression, and clustering. Additionally, the framework introduces a novel attention mechanism to balance self-exploitation (focus on learning source task), and cross-exploration (encourage learning from other tasks). Furthermore, M3H provides explainability insights on how joint learning of additional tasks impacts the learning of source task using a proposed TIM score, shedding light into the dynamics of task interdependencies. Its adaptable architecture facilitates the easy customization and integration of new tasks and data modalities, establishing it as a robust and scalable candidate solution for advancing AI-driven healthcare systems.

Introduction

The integration of Artificial Intelligence (AI) and Machine Learning (ML) has seen unprecedented promise to advance healthcare services and to fundamentally improve our understanding of medicine [1, 2]. Leveraging the increasingly accessible patient digital records, multimodal learning incorporates multiple modalities and sources of data input to provide holistic views of patient profiles [3 - 7]. However, beyond the integration of diverse inputs, a combination of outcomes is often further necessary to comprehensively characterize patients. Multitask learning, which leads to performance breakthroughs in natural language processing such as GPT-2 [8], and computer vision [9 - 11], is a natural extension under this premise to simultaneously learn multiple medical tasks to improve model performance across cardiology [12], psychiatry and psychology [13, 14], oncology [15], radiology [16] and other healthcare domains [17 - 19]. Importantly, multimodal

multitasking emulates existing collaborative efforts in clinical settings, where physicians and administrators across multiple departments often integrate diverse sources of information to jointly navigate multiple complex medical decisions simultaneously.

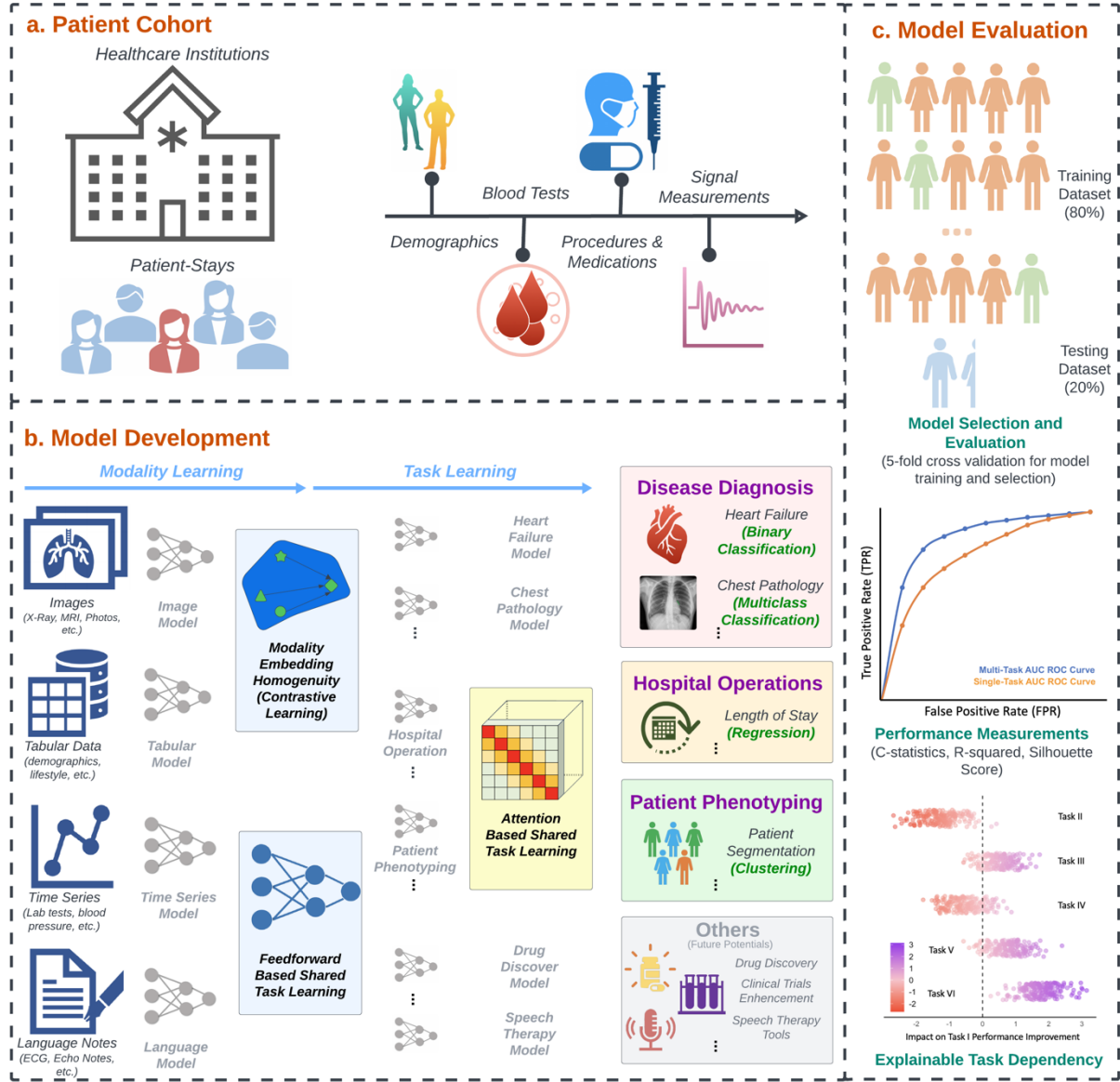


Figure 1. Multimodal Multitask Machine Learning for Healthcare (M3H) framework. Under this framework, users can define the specific input modality as well as outcome tasks they want to jointly learn.

However, it remains challenging to develop an integrative multimodal multitask machine learning framework that is consistently applicable across distinct healthcare domains and machine learning problem classes, while maintaining efficiency in handling increasingly large healthcare datasets [20]. In this work, we introduce M3H (Multimodal Multitask Machine Learning for Healthcare), an explainable, modular framework that integrates task learnings of different healthcare domains: disease diagnoses, healthcare operations, and patient phenotyping, as well as machine learning problem classes: supervised (binary classification, multiclass classification, regression) and

unsupervised (clustering). We demonstrate across 41 medical tasks, and thousands of trained and validated models, significant performance improvements (on average 11.4%) of the M3H framework over traditional single-task models. The M3H framework, in addition to unifying and extending existing medical multimodal multitask learning frameworks, introduces a novel attention mechanism for explicit cross-task learning. It is also designed to be easily adaptable to prototype new user-defined medical tasks, as well as substituting existing modality-specific and task-specific models for user-preferred architecture. Most importantly, to our knowledge, M3H provides the first detailed explainable task-dependency understanding, via task interaction measurement (TIM) score, which systematically investigates and quantifies the value of learning additional task combinations and provides a channel into understanding how learning different medical tasks interplay with one another.

Results

Overview of the M3H framework

M3H (Fig 1.) is developed as a generalizable and explainable framework that leverages multimodal multitask machine learning to improve medical task performance and task-dependency understanding. Qualitatively, M3H improves previous works in this field [12 - 19] by providing an integrated pipeline across a diverse set of tasks both medically (diagnosis, operations, and phenotyping) and methodologically (binary classification, multiclass classification, regression, and clustering), and provides explainability not only on the contribution of input features but on the output task interactions. It further proposes a novel attention mechanism to facilitate cross-task learning.

The M3H framework is developed as an end-to-end framework for integrating multimodal data feature extraction and multitask outcome learnings. To leverage the strong performance of existing state-of-the-art (SOTA) models, M3H first obtains fixed modality-specific embeddings through publicly available, pre-trained models including ClinicalBERT [21] for natural language, and DenseNet121-res224-chex [22] for images. These task-agnostic, not-trainable multimodal embeddings are then passed through further modality-specific learnable feedforward networks and then integrated into a shared-task learning module. In this module, we conduct (i) contrastive learning and (ii) shared-task learning, where the first aims to project embeddings from different modalities into a consistent embedding space, and the second serves as an over-arching tunnel that all tasks must contribute to learning and a proxy for a universal embedding that is relevant for all tasks. We then feed the shared-learned embedding to task-specific networks, which focuses on the learning of each individual task. Finally, these task-specific embeddings integrate knowledge from other task embeddings before making their final predictions, via the cross-task attention mechanism.

Unifying multimodal multitask machine learning problems can be challenging due to the presence of different output spaces (continuous numeric, discrete categories) and the complexity of including a diverse pool of outcomes. M3H integrates tasks of different medical domains and machine learning problem classes by unifying losses from each sub-problem into a single objective function. Specifically, the overall loss is a combination of contrastive loss between multimodal

inputs, and aggregated problem class loss of jointly learned outcomes. During training, updates of the network are made by optimizing each individual loss sequentially.

The M3H framework also provides explainability of task-dependency by computing a task interaction measurement (TIM) score, which measures how joint training of additional tasks affects the performance of the source task. It helps identify tasks that should be trained together to improve performance and provide qualitative medical insights into how medical knowledge interacts and potentially connects.

We demonstrate the feasibility of the proposed M3H framework through its application to a pre-established and validated multimodal dataset. The dataset contains a total of 34,537 samples spanning 7279 hospital stays of 6485 unique patients. The dataset integrates 4 distinct types of input modalities (tabular, time-series, language, and vision), and 11 data sources (for example, echocardiogram notes) with the feature count from each modality summarized in Table 1.

Across 16 disease groupings with 37 disease diagnoses, 3 hospital operations tasks (length of stay, general mortality, and hospital-acquired infection), and 1 patient phenotyping task, the M3H framework demonstrates consistent performance improvement over single-task models. We report the percentage of improvement, as well as its lower and upper bound accounting for standard deviation after applying bootstrapping on the out-of-sample test scores between the best-performing single-task models and best-performing multi-task models in Fig 2. The M3H framework improves performance scores in diagnosis (1.1% - 34.3%), in hospital operations (3.7% – 10.1%), and in patient phenotyping (37.2%). Specifically, the improvement across disease groupings or hospital functionalities include hospital operations ($\Delta_{AUROC} = 4.9\text{-}10.1\%$, $\Delta_{R\text{-squared}} = 3.7\%$), thoracic testing ($\Delta_{\text{Average AUROC}} = 2.6\%$), blood disorder ($\Delta_{AUROC} = 9.2\%$), cardiovascular medicine ($\Delta_{AUROC} = 1.1\text{-}3.8\%$), critical care ($\Delta_{AUROC} = 1.1\text{-}7.4\%$), endocrinology ($\Delta_{AUROC} = 2.3\text{-}8.7\%$), gastroenterology and hepatology ($\Delta_{AUROC} = 2.2\text{-}28.4\%$), infectious diseases ($\Delta_{AUROC} = 5.7\text{-}34.3\%$), internal medicine ($\Delta_{AUROC} = 28.4\%$), nephrology ($\Delta_{AUROC} = 3.4\%$), neurology ($\Delta_{AUROC} = 3.1\text{-}7.2\%$), oncology ($\Delta_{AUROC} = 11.7\text{-}19.5\%$), ophthalmology ($\Delta_{AUROC} = 3.3\text{-}10.5\%$), psychiatry and psychology ($\Delta_{AUROC} = 13.8\text{-}21.9\%$), pulmonary diseases ($\Delta_{AUROC} = 4.8\text{-}8.2\%$), rheumatology ($\Delta_{AUROC} = 9.1\text{-}16.3\%$), and urology ($\Delta_{AUROC} = 6.0\%$).

M3H improves task interdependency understanding.

In previous explainable multitask frameworks for learning biomedical tasks, the focus has remained predominantly on explaining the contribution of input features on each outcome task [19, 23, 24]. However, multitask learning offers a unique perspective that lies in the deep knowledge of understanding how jointly learned tasks interact with each other. The majority of past multitask works in healthcare rely on prior medical knowledge that learning specific task combinations is beneficial to each problem. This approach heavily relies on expert understanding of the specific domain studied and thus introduces a need for a rigorous procedure to demonstrate why tasks are selected to be combined.

Additionally, there has been an increase in interest in bridging understanding of medicine across different medical domains. We show in Fig. 3 that using the proposed task interaction measurement (TIM) score, we can quantify both the positive and negative contribution of additional tasks on a source task. Of particular note, consistent with previous findings, the additional joint learning of infectious diseases (bacterial intestinal infections, antimicrobial resistance, HIV, Hepatitis BC,

tuberculosis) helps improve the learning of anemia (average $\Delta_{AUROC} = 2\%$) [25], as is the case of inflammatory bowel disease learning contributing to bipolar disorder risk prediction ($\Delta_{AUROC} = 5\%$) [26].

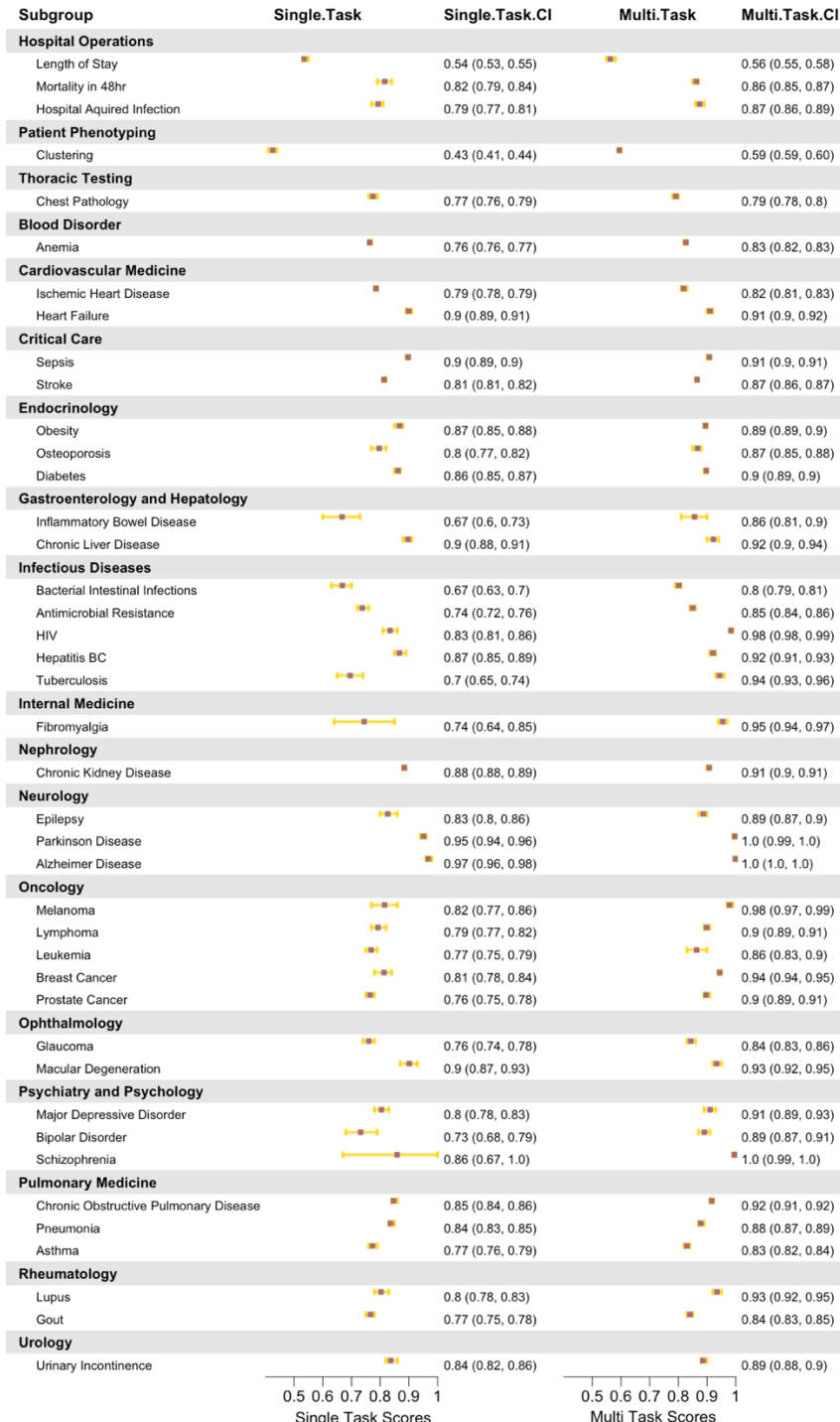


Figure 2. Performance of the M3H framework across all important domains of healthcare tasks and disease groupings.

Overall, the TIM score helps understanding whether a particular task combination improves individual learning by sharing knowledge, or impairs learning by competing between conflictive objectives, and can provide qualitative insights to better understand potentially under-investigated medical outcome connections.

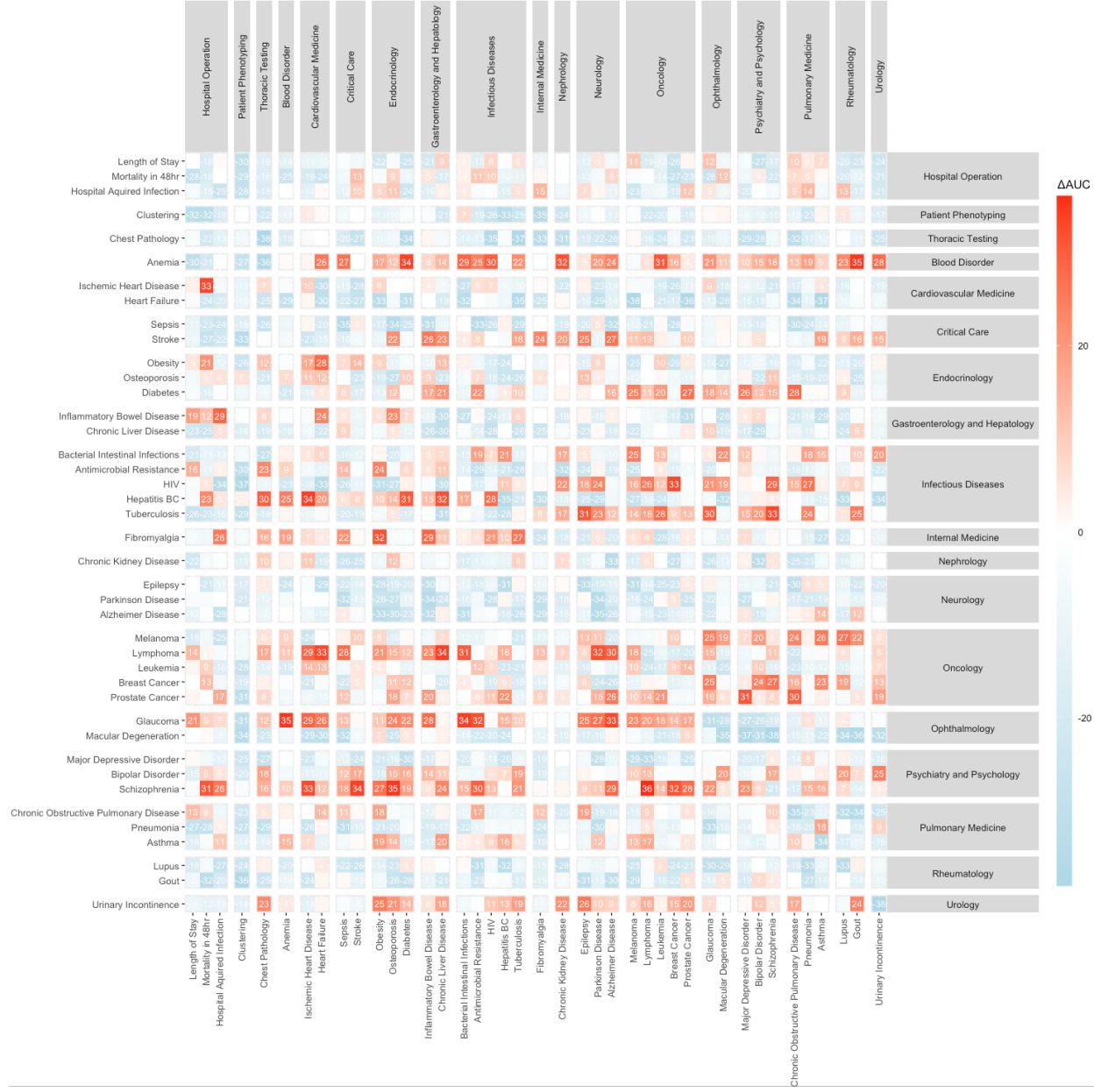


Figure 3. Heatmap of all TIM scores across all tasks. We consider the comparison between all task combinations of size 2, and single source task for computational efficiency.

M3H is generalizable across machine learning problem classes.

Machine learning (ML) can be generally classified as supervised learning and unsupervised learning, with each problem class having unique modeling techniques tailored for various outcomes and objectives. However, the distinction of machine learning problem class should not

pose barriers to integrating relevant tasks that can benefit from learning simultaneously. In M3H, we unify the learning of the most commonly used problem classes in healthcare: binary classification, multiclass classification, regression, and clustering, into a single framework. We show in Fig. 4 that joint learning across machine learning problem classes improves both quantitative performance as well as qualitative understanding of the source tasks. In particular, for binary classification, predicted major depressive disorder risk scores quantile, when compared against observed event rate, shows more consistency between female and male subgroups under the multitask setting; for multiclass classification, we observe reduced variability of ROC curve across different thorax conditions with higher averaged AUROC measure; for regression, multitask captures tail-predictions (extended length of stay) slightly more comprehensively than single-task; for clustering, post-UMAP (Uniform Manifold Approximation and Projection) processing demonstrates significantly more distinct boundaries between clusters and structural patterns in the multitask setting.

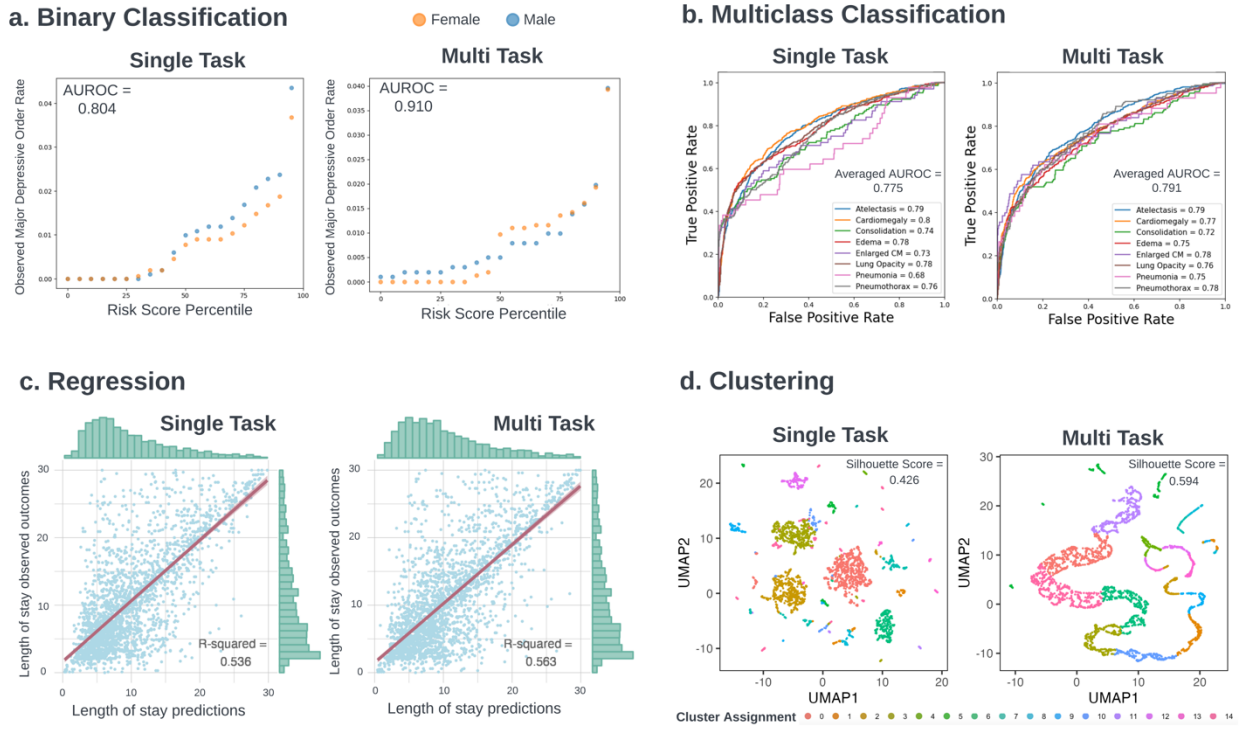


Figure 4. MultiTask outperforms SingleTask across four most studied machine learning problem classes.

Discussion

Standardized and large-scale EHR data, now increasingly accessible across medical departments, offers an unprecedented opportunity to enhance predictive analytics, tailor personalized treatment plans, streamline administrative processes, and ultimately improve the quality of patient care. Our comprehensive analysis underscores the advantage of integrating diverse data modalities and learning multiple tasks simultaneously, presenting it as a unifying approach to developing multimodal multitask protocols for healthcare. The implementation of shared multitask learning across different medical domains from cohesive, individualized patient profiles provides healthcare systems the opportunity to apply the M3H framework for the rapid development of

scalable AI prototypes. With proper validation, these prototypes are not only applicable in clinical decision-making processes but also in managing administrative operations. The M3H framework specially addresses several bottleneck challenges in this setting, including the difficulty of integration across multiple distinct machine learning problem classes into a single framework, and the lack of explainability metrics to measure how and why combining certain tasks improves performance. In particular, the M3H framework complements and extends previous literature on the topic, and provides new perspectives on the following aspects:

- (A) First, M3H provides the first attempt to consolidate healthcare tasks beyond multi-disease diagnosis to hospital operations and patient phenotyping within a single system. This innovative approach is underscored by its potential to encompass not only clinical, but also operational and biological dynamics of patient care, and to offer a comprehensive understanding across the healthcare continuum. Furthermore, M3H facilitates integration between diverse machine learning problem classes, from supervised binary classification, multiclass classification, and regression to unsupervised clustering. This versatility establishes unparalleled access and flexibility for both physicians and healthcare practitioners to combine distinct analytical tasks regardless of boundaries posed by technical definitions of the original problem of interest.
- (B) Second, M3H introduces the TIM score, an explainable metric designed to measure the incremental performance benefits from training additional tasks in conjunction with the source task. While previous studies in this field rely on *a priori* assumptions or medical observations to demonstrate the quantitative and qualitative advantage of multitask learning for the investigated domain, using the TIM score, M3H provides a novel explainable mechanism that systematically quantifies the value of adding additional jointly learned tasks in more rigorous level of granularity and broader combinatorial outcome space than any prior studies. Our extensive testing, which includes model experimentations across 37 disease diagnoses, three hospital operation tasks, and one patient phenotyping task, provides robust empirical evidence supporting the notion that multitask training can enhance the performance of single-task models, provided that the task combinations are judiciously chosen. Conversely, our findings also reveal previously unreported phenomena where certain joint training diminishes the analytical gain of the canonical models. This highlights the existence of competing objectives and underscores the necessity of a thorough exploration of the dynamics of task interactions, a process facilitated by the TIM score and its associated analyses.
- (C) Finally, M3H develops a novel cross-task attention mechanism that explicitly models the learning between medical tasks by balancing self-exploitation (focus on learning source task) and cross-exploration (encourage learning from other tasks). The uniquely structured attention method is tailored for the understanding of complex interdependencies among various medical tasks, enabling a more adaptive and effective approach to collaborative learning. The attention mechanism not only optimizes the learning process across different tasks but also enhances the overall capability to draw relevant and actionable insights by providing an attention weight,

an explicit quantification of how much each task is contributing to the learning of another, allowing direct access to the decision mechanism of multitask learning.

M3H is provided to both clinicians and researchers to develop multimodal multitask AI systems that are adapted to the patient cohorts, available data modalities, and targeted medical tasks of interest. The modular architecture for pre-trained feature extractors, modality-specific networks, and task-specific networks is designed to encourage user-defined modifications and replacements for their research objectives. The ease-to-implement nature of the M3H framework is intended to streamline the application and future deployment of impactful AI systems, which are poised to drive clinical impacts and healthcare transformations. We hope the framework can assist and support physicians in building a unified framework that accelerates system development while offering novel insights into the understanding and management of clinical and operational activities in healthcare organizations.

Methods

Dataset and Patient representation

HAIM-MIMIC-MM [3] is a patient-centric dataset derived from Medical Information Mart for Intensive Care IV (MIMIC-IV) [28], a public electronic health record database from Beth Israel Deaconess Medical Center containing de-identified records of all patients admitted to the intensive care unit (ICU) between 2008-2019. HAIM-MIMIC-MM offers access to contemporary, large-scale patient cohorts with modular constituent data organization, and most importantly, integrates multiple modalities of data inputs into a single database, ranging from demographics, chart events, laboratory events, procedure events, radiological notes, electrocardiogram notes, echo-cardiogram notes, as well as chest X-Ray images. Specifically, HAIM-MIMIC-MM aggregates all available medical information of a patient's hospital admission-stay occurring before the discharge or death time, with their details summarized in Table 1. Fixed-size vector representation (embeddings) of data from four modalities: tabular (dimension of 6), time-series (dimension of 451), vision (dimension of 2084), and language (dimension of 2304), are extracted using pre-trained, state-of-the-arts models and combined into a comprehensive multimodal patient representation.

Each sample within the HAIM-MIMIC-MM dataset corresponds to all prior patient information from the time of admission until an inference event, including the time of imaging procedure for pathology diagnosis, the 48-hour window for mortality prediction, or the end of hospital stay. The rich patient profile developed in HAIM-MIMIC-MM allows for standardized, fast prototyping of relevant healthcare models.

Table 1. Feature characteristics of the HAIM-MIMIC-MM database

Modality	Source	# of Features
Tabular	Demographics	6
Time Series	Chart Event	99
	Lab Events	242
	Procedure Events	110

Language	Radiological Notes	768
	Electrocardiogram Notes	768
	Echo-cardiogram Notes	768
Vision	Chest X-ray images	2304

HAIM-MIMIC-MM is a combined multimodal dataset that contains both the MIMIC-IV and MIMIC Chest X-Ray images dataset that only include patients that have at least one chest X-ray performed.

Medical Tasks of Interest

Disease Diagnosis

Early prediction of disease diagnosis is one of the most important and studied areas of healthcare due to its crucial role in enabling timely intervention to reduce severe complications and improve treatment success. It is particularly important to note an increasing interest across medical fields to try to understand connections between diseases across different medical domains, ranging from the discovery of the connection between gut microbiome and Alzheimer's to diabetes and heart diseases [31, 32]. In this study, we identified 37 commonly known conditions and diseases and grouped them into 15 clinical departments based on the Mayo Clinic disease and condition directory.

Specifically, we cover departments ranging from blood disorders, cardiovascular medicine, critical care, endocrinology, gastroenterology and hepatology, infectious diseases, nephrology, neurology, oncology, ophthalmology, psychiatry and psychology, pulmonary diseases, rheumatology, and urology. Identification of each specific disease diagnosis is summarized in Supplemental Table 1, and we structure the problem as binary classification: identified ICD code is recorded in the patient's end-of-hospital discharge diagnosis record (1), otherwise (0).

In addition to disease diagnosis, we also consider chest pathology diagnosis, which is structured as a multiclass problem with 8 common thoraces diseases: atelectasis, cardiomegaly, consolidation, edema, enlarged cardio mediastinum (enlarged CM), lung opacity, pneumonia, pneumothorax. Patient is included only if they have a single and unique pathology identified as positive, to avoid overlapping between outcome classes. The pathologies are selected so that no single pathology occupies less than 1% of the entire patient population or contributes to a significant reduction of data sample size.

Hospital Operations

The daily operations of healthcare facilities have profound implications on their resource allocation, patient satisfaction, as well as clinician decision effectiveness and timeliness. Specifically, patient flow forecast (length of stay prediction) allows the logistics team to get advanced notice of discharge, ultimately improves patient quality of care and reduces operational costs in the hospital system; deterioration warnings (mortality in the next 48 hours prediction), especially in time-sensitive environment such as ICU units, guides physicians to make rapid, yet critical decisions in a data-intensive environment [33]; safety enhancement (hospital-acquired infection prediction) prevents infection outbreaks with

targeted control practices to safeguard patient health, incentivizing facilities to follow hygiene and sterilization protocols to avoid operational costs [34].

We structure the length of stay prediction as a regression problem (unit of days), mortality prediction, and HAI prediction as binary classification problems. Specifically, following previous literature [35], we identify catheter-related bloodstream infections, nosocomial pneumonia, surgical site infections, and urinary tract infections as HAI infections.

Patient Phenotyping

As medical records become more standardized, recorded data may be structured in ways that are best suited for reimbursement and billing purposes. Such imposed bias could potentially miss clinical information that misclassifies patients into irrelevant patient subgroups. Patient phenotyping provides an important perspective into understanding additional structures shared by patient subgroups not traditionally defined. In our work, we look for the best patient grouping mechanism that groups the cohort into 15 phenotypes via clustering.

Machine Learning (ML) Class of Problem

Supervised-Binary Classification

Binary classification is the most widely used form of problem class in healthcare and refers to the prediction of two classes of outcomes: positive and negative. In settings where only 2 discrete outcomes are present (i.e., infected or not), or where a clear numerical cutoff indicates a difference in condition (i.e., death after 48 hours), we use binary classification to understand the variable relationship and evaluate the performance using the area under the receiver operating curve (AUROC). Specifically, for tasks with overly imbalanced classes (positive sample less than 10% of cohort), we initialize the output layer's bias as $\log(n_{positive}/n_{negative})$ to de-bias the imbalance following previous literature[37].

Supervised-Multiclass Classification

Multiclass classification refers to the prediction of multiple classes of related outcomes and is studied when inherent structures between classes are present and related, including device-specific identifications [39] and anatomic-specific disease detections [40 - 42]. Due to the natural imbalance of certain class outcomes, we evaluate it by computing the averaged AUROC across all classes.

Supervised-Regression

Regression problem refers to the predictive modeling of continuous numerical outcomes. It is especially important when the prediction of the exact values is cost-sensitive, which has a large impact on care access fairness [43], operational efficiency [44], and physician wellness [45]. R-squared value is chosen as the evaluation metric for regression-related problems.

Unsupervised-Clustering

Clustering problems are fundamental in exploratory efforts to understand data structures without applying pre-determined labels for training [46], as well as anomaly detection for

healthcare fraud prevention [47]. A high-quality cluster assignment achieves a high silhouette score, an evaluation of both separability, the ability to distinguish clusters from one another, and homogeneity, the ability to have consistent content within each cluster.

M3H Architecture Design

The M3H framework assigns a pre-defined modality-specific feedforward network for each input modality and a task-specific network for each outcome task, with details in Supplemental Figure 2. The two novel designs on clustering and cross-task attention mechanism are explained below, with illustration in Figure 4.

Clustering

As an unsupervised problem with no access to true labels, clustering poses a unique challenge when integrated into the pipeline. To effectively group patients into different phenotypes, we train an autoencoder that learns accurate low-dimensional latent space that can be then clustered into groups via traditional methods such as K-means clustering. The autoencoder architecture can be found in the Supplemental Fig. 2.

Specifically, we first concatenate all embeddings from all modalities into an aggregated embedding, this embedding is then fed during training into an autoencoder to compress the original feature space into low-dimension latent space and then re-expanded back to the original dimensions. A good quality latent space aims to achieve low reconstruction loss, measuring a low difference between the encoder input and the decoder output of the autoencoder. The learned latent space is then clustered into 15 patient subgroups and evaluated for quality.

Cross-Task Attention for Knowledge Sharing

Attention mechanism [48] is at the foundation of recent breakthroughs in artificial intelligence. At its core, attention is constructed by variations of the key, query, and value vectors to capture interactions between its inputs. Attention mechanism is well-positioned to exploit dependencies between tasks: by projecting each task’s embeddings as a token, we can leverage the attention mechanism to enable explicit task knowledge sharing. A detailed algorithm outline of the novel cross-task attention computation can be found in Supplemental Fig. 4.

Following traditional practice, input to obtain the key and value vectors is the original task embedding $x_s \in \mathbb{R}^{n_{batch} \times n_{tasks} \times n_{feature}}$ from jointly-learning of a specified set of task s , where n_{batch} refers to the number of samples passed through each learning iteration (batch size), $n_{feature}$ refers to the number of features generated to encode knowledge for each task, and n_{tasks} refers to the number of tasks in s . However, we aim to find a universal mapping between task tokens indicating the index of a task, with the embedding that best represents a task. This calls for a query vector that is independent of the batch update. To do so, we generate the query embedding via mapping of the task tokens vector T_s to task embeddings via a linear projection $Q_s = f(T_s): \mathbb{N}^{n_{tasks}} \rightarrow \mathbb{R}^{n_{tasks} \times n_{feature}}$. Finally, we apply linear projections to all embeddings to improve representation quality, and obtain query vector $Q_s \in \mathbb{R}^{n_{tasks} \times n_{feature}}$, key vector $K_s \in \mathbb{R}^{n_{batch} \times n_{tasks} \times n_{feature}}$, and value vector $V_s \in \mathbb{R}^{n_{batch} \times n_{tasks} \times n_{feature}}$.

The product of the computed query and key vectors, referred to as attention weight, indicates the relevance or emphasis put on a specific token in the value vector. We aim to find a balance between exploiting self-learning (reusing knowledge from the original task) while exploring cross-learning (incorporating knowledge from other unrelated tasks) in a controlled manner. This balance is achieved by adapting the initial attention weight $M_s \in \mathbb{R}^{n_{batch} \times n_{tasks} \times n_{tasks}}$ through the projection $W_s = \text{softmax}(I_s + \frac{\alpha M_s}{\max(M_s)})$, where $I_s \in \mathbb{R}^{n_{batch} \times n_{tasks} \times n_{tasks}}$ is the identity matrix encouraging self-learning, and α is the strength of exploration encouraging cross task learning. This attention weight is then applied to the values vector to obtain the final cross-learned task embeddings.

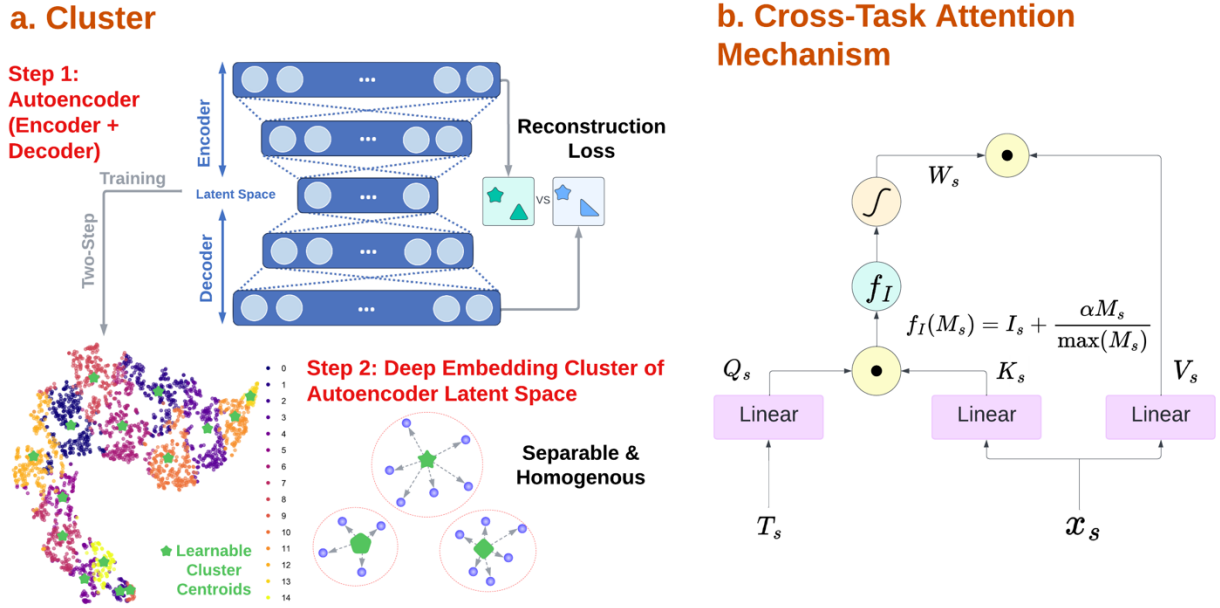


Figure 5. Architecture design of the clustering and cross-task attention mechanism. a) Two-step approach for clustering. b) Cross-task attention mechanism, with linear projections and balancing of self-exploitation and cross-exploration.

Model Loss

The aggregated loss used to train the network is defined as a weighted average across all losses: $l_{total} = w_c l_{constrative} + \sum_{t \in B_s} w_t l_{binary,s} + \sum_{t \in M_s} w_t l_{multiclass} + \sum_{t \in R_s} w_t l_{regression} + \sum_{t \in C_s} w_t l_{cluster}$ where w_c, w_t refers to the weight assigned for contrastive loss and task t , B_s, M_s, R_s, C_s refers to the sets of tasks that are in the binary, multiclass, regression and cluster problem classes. Specifically, binary classification loss refers to binary cross entropy loss; multiclass classification loss refers to negative log-likelihood loss; regression loss refers to mean absolute error loss; cluster reconstruction loss refers to the mean squared error between encoder input and decoder output. All weights have been initialized to 1 for ease of implementation.

Task Interaction Measurement (TIM) Score

Across the literature on multitask applications in healthcare, the majority of the work on explainability focused on the quantification of input feature contribution to task predictions. We point out in this work that it is also critical to understand how different tasks interact and depend on each other when jointly learned. We propose a task interaction measurement (TIM) score, computed as the difference in performance scores between joint learning of task pairs and source-task learning. Given M as the number of all possible tasks, S as a set of tasks that do not contain either task i or task j , and $\tilde{f}_x(S \cup \{i\})$ as a function of performance score of task i given features x and joint learning all tasks belonging to S and task i , we define TIM as follows:

$$\delta_{ij} = \frac{1}{2^{M-2}} \sum_{S \subseteq \{i,j\}} \tilde{f}_x(S \cup \{i,j\}) - \tilde{f}_x(S \cup \{i\})$$

As the number of all possible tasks grows, this score requires an exponentially increasing number of all potential task combinations of S . In practice, to avoid computational hurdles, we can either sample a subset of potential S to obtain an approximation of the true TIM score or restrict the number of task pair sizes to be small (i.e., smaller than 5).

Model Training Pipeline

We initially explored various feedforward architectures for each modality-specific and task-specific network including different activation functions (ReLU, Sigmoid, Tanh), dropout layers, normalization layers, different optimizers (RMSprop, SGD, Momentum, Adam), and gradient clipping. The canonical architecture used in all following experiments was selected to support GPU optimization for computational efficiency (i.e., the number of filters in layers mostly are multiples of 64) and was shown to have a consistently superior performance during preliminary investigations. The rescaling coefficient in the cross-task attention mechanism α is set to be 0.1 as it is explored to be a stable point between performance stability and efficient learning.

We first split the dataset into 80% training and 20% testing by stratifying on a patient level to ensure no data leakage between training and testing for all model training or validation processes. We then apply a 5-fold cross-validation on the training set to select the best combinations of batch size (256, 512) and learning rate (0.0005, 0.001). Specifically, within each run of 15 epochs, 4 of the 5 folds are used for model training, and the remaining one is used for validation. The average of all 5 validation scores across all tasks will be computed for each hyperparameter combination, and a final model will be trained on the entire training set on the hyperparameter combination with the highest average validation score.

As the number of tasks included in joint learning grows, there is an exponentially growing number of potential possible task pair combinations. We consider the following task selection procedure to optimize our likelihood of locating the best-performing multitask model: given a set of tasks $s \cup \{i\}$ and its performance on i , we conduct experiments on all possible $s \cup \{i\} \cup \{j\}$ where j is a task not previously included. We only keep the best-performing top 3 such pairs, and iteratively repeat this process until no further improvements are observed. The final combination is the optimal task combination that can be used to improve task performance for a specific task.

All computational experiments are conducted in MIT's Supercloud Computing server using the NVIDIA Tesla V100 Volta graphics processing unit. Job submissions have been optimized for hardware architecture and node scheduling.

DATA AVAILABILITY

MIMIC-IV data is available (<https://physionet.org/content/mimiciv/2.2/>), and code to generate the HAIM-MIMIC-MM dataset is also available (<https://physionet.org/content/haim-multimodal/1.0.0/>).

CODE AVAILABILITY

The codes used for this study can be made available by contacting the corresponding author. Access to codes will be granted for requests for academic use within four weeks of application. R and Python are required software to use the code.

REFERENCES

[1] Topol, E. Deep medicine: how artificial intelligence can make healthcare human again. (Hachette UK, 2019).

[2] Yu, K., Beam, A. L., & Kohane, I. S. (2018). Artificial intelligence in healthcare. *Nature Biomedical Engineering*, 2(10), 719-731. <https://doi.org/10.1038/s41551-018-0305-z>

[3] Soenksen, L. R., Ma, Y., Zeng, C., Boussioux, L., Villalobos Carballo, K., Na, L., Wiberg, H. M., Li, M. L., Fuentes, I., & Bertsimas, D. (2022). Integrated multimodal artificial intelligence framework for healthcare applications. *Npj Digital Medicine*, 5(1), 1-10. <https://doi.org/10.1038/s41746-022-00689-4>

[4] Huang, S.-C., Pareek, A., Seyyedi, S., Banerjee, I. & Lungren, M. P. Fusion of medical imaging and electronic health records using deep learning: a systematic review and implementation guidelines. *NPJ Dig. Med.* 3, 1–9 (2020).

[5] Acosta, J. N., Falcone, G. J., Rajpurkar, P., & Topol, E. J. (2022). Multimodal biomedical AI. *Nature Medicine*, 28(9), 1773-1784. <https://doi.org/10.1038/s41591-022-01981-2>

[6] Tadas Baltrusaitis, Chaitanya Ahuja, and Louis-Philippe Morency. 2019. Multimodal Machine Learning: A Survey and Taxonomy. *IEEE Trans. Pattern Anal. Mach. Intell.* 41, 2 (February 2019), 423–443. <https://doi.org/10.1109/TPAMI.2018.2798607>

[7] Ahmed Z, Mohamed K, Zeeshan S, Dong X. Artificial intelligence with multi-functional machine learning platform development for better healthcare and precision medicine. *Database (Oxford)*. 2020 Jan 1;2020:baaa010. doi: 10.1093/database/baaa010. PMID: 32185396; PMCID: PMC7078068.

[8] Radford, Alec, Jeff Wu, Rewon Child, David Luan, Dario Amodei and Ilya Sutskever. “Language Models are Unsupervised Multitask Learners.” (2019).

[9] Ren, S., He, K., Girshick, R., & Sun, J. (2015). Faster r-cnn: Towards real-time object detection with region proposal networks. *Advances in Neural Information Processing Systems*, 28.

[10] He, K., Gkioxari, G., Dollár, P., & Girshick, R.B. (2017). Mask R-CNN. *2017 IEEE International Conference on Computer Vision (ICCV)*, 2980-2988.

[11] Reed, S., Zolna, K., Parisotto, E., Colmenarejo, S. G., Novikov, A., Gimenez, M., Sulsky, Y., Kay, J., Springenberg, J. T., Eccles, T., Bruce, J., Razavi, A., Edwards, A., Heess, N., Chen, Y., Hadsell, R., Vinyals, O., Bordbar, M., & De Freitas, N. (2022). A Generalist Agent. *ArXiv*. /abs/2205.06175

[12] Torres-Soto, J., Ashley, E.A. Multi-task deep learning for cardiac rhythm detection in wearable devices. *npj Digit. Med.* 3, 116 (2020). <https://doi.org/10.1038/s41746-020-00320-4>

[13] Tseng, V.W.S., Sano, A., Ben-Zeev, D. *et al.* Using behavioral rhythms and multi-task learning to predict fine-grained symptoms of schizophrenia. *Sci Rep* **10**, 15100 (2020). <https://doi.org/10.1038/s41598-020-71689-1>

[14] Lee, M.H., Kim, N., Yoo, J. *et al.* Multitask fMRI and machine learning approach improve prediction of differential brain activity pattern in patients with insomnia disorder. *Sci Rep* **11**, 9402 (2021). <https://doi.org/10.1038/s41598-021-88845-w>

[15] Fu, S., Lai, H., Li, Q., Liu, Y., Zhang, J., Huang, J., Chen, X., Duan, C., Li, X., Wang, T., He, X., Yan, J., Lu, L., & Huang, M. (2021). Multi-task deep learning network to predict future macrovascular invasion in hepatocellular carcinoma. In eClinicalMedicine (Vol. 42, p. 101201). Elsevier BV. <https://doi.org/10.1016/j.eclim.2021.101201>

[16] Jin, C., Yu, H., Ke, J. *et al.* Predicting treatment response from longitudinal images using multi-task deep learning. *Nat Commun* **12**, 1851 (2021). <https://doi.org/10.1038/s41467-021-22188-y>

[17] Eyuboglu, S., Angus, G., Patel, B.N. *et al.* Multi-task weak supervision enables anatomically-resolved abnormality detection in whole-body FDG-PET/CT. *Nat Commun* **12**, 1880 (2021). <https://doi.org/10.1038/s41467-021-22018-1>

[18] Wang, X., Cheng, Y., Yang, Y. *et al.* Multitask joint strategies of self-supervised representation learning on biomedical networks for drug discovery. *Nat Mach Intell* **5**, 445–456 (2023). <https://doi.org/10.1038/s42256-023-00640-6>

[19] Tang, X., Zhang, J., He, Y. *et al.* Explainable multi-task learning for multi-modality biological data analysis. *Nat Commun* **14**, 2546 (2023). <https://doi.org/10.1038/s41467-023-37477-x>

[20] A. Ahmed, R. Xi, M. Hou, S. A. Shah and S. Hameed, "Harnessing Big Data Analytics for Healthcare: A Comprehensive Review of Frameworks, Implications, Applications, and Impacts," in *IEEE Access*, vol. 11, pp. 112891-112928, 2023, doi: 10.1109/ACCESS.2023.3323574.

[21] Alsentzer, E., Murphy, J. R., Boag, W., Weng, W., Jin, D., Naumann, T., & McDermott, M. B. (2019). Publicly Available Clinical BERT Embeddings. *ArXiv*. /abs/1904.03323

[22] Cohen, J. P., Viviano, J. D., Bertin, P., Morrison, P., Torabian, P., Guarrrera, M., Lungren, M. P., Chaudhari, A., Brooks, R., Hashir, M., & Bertrand, H. (2021). TorchXRayVision: A library of chest X-ray datasets and models. *ArXiv*. /abs/2111.00595

[23] Malhotra A, Mittal S, Majumdar P, Chhabra S, Thakral K, Vatsa M, Singh R, Chaudhury S, Pudrod A, Agrawal A. Multi-task driven explainable diagnosis of COVID-19 using chest X-ray images. *Pattern Recognit*. 2022 Feb;122:108243. doi: 10.1016/j.patcog.2021.108243. Epub 2021 Aug 21. PMID: 34456368; PMCID: PMC8379001.

[24] Shickel, B., Loftus, T.J., Ruppert, M. *et al.* Dynamic predictions of postoperative complications from explainable, uncertainty-aware, and multi-task deep neural networks. *Sci Rep* **13**, 1224 (2023). <https://doi.org/10.1038/s41598-023-27418-5>

[25] Means, R. T. (2000). The anaemia of infection. *Best Practice & Research Clinical Haematology*, **13**(2), 151-162. <https://doi.org/10.1053/beha.1999.0065>

[26] McGuinness, A.J., Davis, J.A., Dawson, S.L. *et al.* A systematic review of gut microbiota composition in observational studies of major depressive disorder, bipolar disorder and schizophrenia. *Mol Psychiatry* **27**, 1920–1935 (2022). <https://doi.org/10.1038/s41380-022-01456-3>

[27] Engels EA, Brock MV, Chen J, Hooker CM, Gillison M, Moore RD. Elevated incidence of lung cancer among HIV-infected individuals. *J Clin Oncol*. 2006 Mar 20;24(9):1383-8. doi: 10.1200/JCO.2005.03.4413. PMID: 16549832.

[28] Johnson, A. E., Bulgarelli, L., Shen, L., Gayles, A., Shammout, A., Horng, S., Pollard, T. J., Hao, S., Moody, B., Gow, B., Lehman, L., Celi, L. A., & Mark, R. G. (2023). MIMIC-IV, a freely accessible electronic health record dataset. *Scientific Data*, **10**(1), 1-9. <https://doi.org/10.1038/s41597-022-01899-x>

[29] Singh, A. V., Chandrasekar, V., Paudel, N., Laux, P., Luch, A., Gemmati, D., Tisato, V., Prabhu, K. S., Uddin, S., & Dakua, S. P. (2023). Integrative toxicogenomics: Advancing precision medicine and toxicology through artificial intelligence and OMICs technology. *Biomedicine & Pharmacotherapy*, **163**, 114784. <https://doi.org/10.1016/j.biopha.2023.114784>

[30] Singh, A., Randive, S., Breggia, A., Ahmad, B., Christman, R., & Amal, S. (2023). Enhancing Prostate Cancer Diagnosis with a Novel Artificial Intelligence-Based Web Application: Synergizing Deep Learning Models, Multimodal Data, and Insights from Usability Study with Pathologists. *Cancers*, **15**(23), 5659. <https://doi.org/10.3390/cancers15235659s>

[31] Aura L. Ferreiro et al. ,Gut microbiome composition may be an indicator of preclinical Alzheimer's disease. *Sci. Transl. Med.* 15, eabo2984 (2023). DOI: 10.1126/scitranslmed.abo2984

[32] Rawshani A, Rawshani A, Franzén S, Sattar N, Eliasson B, Svensson AM, Zethelius B, Miftaraj M, McGuire DK, Rosengren A, Gudbjörnsdóttir S. Risk Factors, Mortality, and Cardiovascular Outcomes in Patients with Type 2 Diabetes. *N Engl J Med*. 2018 Aug 16;379(7):633-644. doi: 10.1056/NEJMoa1800256. PMID: 30110583.

[33] Na, L., Carballo, K. V., Pauphilet, J., Kombert, D., Castiglione, A., Khalifa, M., Hebbal, P., Stein, B., & Bertsimas, D. (2023). Patient Outcome Predictions Improve Operations at a Large Hospital Network. *ArXiv*. /abs/2305.15629

[34] Peasah SK, McKay NL, Harman JS, Al-Amin M, Cook RL. Medicare non-payment of hospital-acquired infections: infection rates three years post implementation. *Medicare Medicaid*

Res Rev. 2013 Sep 25;3(3):mmrr.003.03.a08. doi: 10.5600/mmrr.003.03.a08. PMID: 24753974; PMCID: PMC3983733.

[35] Ishigami J, Trevisan M, Xu H, Coresh J, Matsushita K, Carrero JJ. Estimated GFR and Hospital-Acquired Infections Following Major Surgery. *Am J Kidney Dis.* 2019 Jan;73(1):11-20. doi: 10.1053/j.ajkd.2018.06.029. Epub 2018 Sep 7. PMID: 30201545.

[36] 1999 - 2022 AHA Annual Survey, Copyright 2022 by Health Forum, LLC, an affiliate of the American Hospital Association. Special data request, 2023.

[37] Martín Abadi, Ashish Agarwal, Paul Barham, Eugene Brevdo, Zhifeng Chen, Craig Citro, Greg S. Corrado, et al. TensorFlow: Large-scale machine learning on heterogeneous systems, 2015.

[38] M. Kampffmeyer, S. Lokse, F. M. Bianchi, L. Livi, A. . -B. Salberg and R. Jenssen, "Deep divergence-based clustering," 2017 IEEE 27th International Workshop on Machine Learning for Signal Processing (MLSP), Tokyo, Japan, 2017, pp. 1-6, doi: 10.1109/MLSP.2017.8168158.

[39] Anguita, D., Ghio, A., Oneto, L., Parra, X., Reyes-Ortiz, J.L. (2012). Human Activity Recognition on Smartphones Using a Multiclass Hardware-Friendly Support Vector Machine. In: Bravo, J., Hervás, R., Rodríguez, M. (eds) Ambient Assisted Living and Home Care. IWAAL 2012. Lecture Notes in Computer Science, vol 7657. Springer, Berlin, Heidelberg. https://doi.org/10.1007/978-3-642-35395-6_30

[40] Konstantin Pogorelov, Kristin Ranheim Randel, Carsten Griwodz, Sigrun Losada Eskeland, Thomas de Lange, Dag Johansen, Concetto Spampinato, Duc-Tien Dang-Nguyen, Mathias Lux, Peter Thelin Schmidt, Michael Riegler, and Pal Halvorsen. 2017. KVASIR: A Multi-Class Image Dataset for Computer Aided Gastrointestinal Disease Detection. <https://doi.org/10.1145/3193289>

[41] Alshmrani, G. M. M., Ni, Q., Jiang, R., Pervaiz, H., & Elshennawy, N. M. (2023). A deep learning architecture for multi-class lung diseases classification using chest X-ray (CXR) images. *Alexandria Engineering Journal*, 64, 923-935. <https://doi.org/10.1016/j.aej.2022.10.053>

[42] Hoang, L., Lee, S., Lee, E., & Kwon, K. (2022). Multiclass Skin Lesion Classification Using a Novel Lightweight Deep Learning Framework for Smart Healthcare. *Applied Sciences*, 12(5), 2677. <https://doi.org/10.3390/app12052677>

[Yuan 2016] Yuan, H., Paskov, I., Paskov, H. *et al.* Multitask learning improves prediction of cancer drug sensitivity. *Sci Rep* 6, 31619 (2016). <https://doi.org/10.1038/srep31619>

[43] Reid KW, Vittinghoff E, Kushel MB. Association between the level of housing instability, economic standing and health care access: a meta-regression. *J Health Care Poor Underserved.* 2008 Nov;19(4):1212-28. doi: 10.1353/hpu.0.0068. PMID: 19029747.

[44] Rich Caruana, Yin Lou, Johannes Gehrke, Paul Koch, Marc Sturm, and Noemie Elhadad. 2015. Intelligible Models for HealthCare: Predicting Pneumonia Risk and Hospital 30-day Readmission. In Proceedings of the 21th ACM SIGKDD International Conference on Knowledge

Discovery and Data Mining (KDD '15). Association for Computing Machinery, New York, NY, USA, 1721–1730. <https://doi.org/10.1145/2783258.2788613>

[45] Salari N, Khazaie H, Hosseini-Far A, Khaledi-Paveh B, Kazeminia M, Mohammadi M, Shohaimi S, Daneshkhah A, Eskandari S. The prevalence of stress, anxiety and depression within front-line healthcare workers caring for COVID-19 patients: a systematic review and meta-regression. *Hum Resour Health.* 2020 Dec 17;18(1):100. doi: 10.1186/s12960-020-00544-1. PMID: 33334335; PMCID: PMC7745176.

[46] Haraty, R. A., Dimishkieh, M., & Masud, M. (2015). An Enhanced k-Means Clustering Algorithm for Pattern Discovery in Healthcare Data. *International Journal of Distributed Sensor Networks.* <https://doi.org/10.1155/2015/615740>

[47] Hillerman, T., Souza, J. C. F., Reis, A. C. B., & Carvalho, R. N. (2017). Applying clustering and AHP methods for evaluating suspect healthcare claims. *Journal of Computational Science, 19*, 97-111. <https://doi.org/10.1016/j.jocs.2017.02.007>

[48] Ashish Vaswani, Noam Shazeer, Niki Parmar, Jakob Uszkoreit, Llion Jones, Aidan N. Gomez, Łukasz Kaiser, and Illia Polosukhin. 2017. Attention is all you need. In Proceedings of the 31st International Conference on Neural Information Processing Systems (NIPS'17). Curran Associates Inc., Red Hook, NY, USA, 6000–6010.

SUPPLEMENTAL MATERIALS

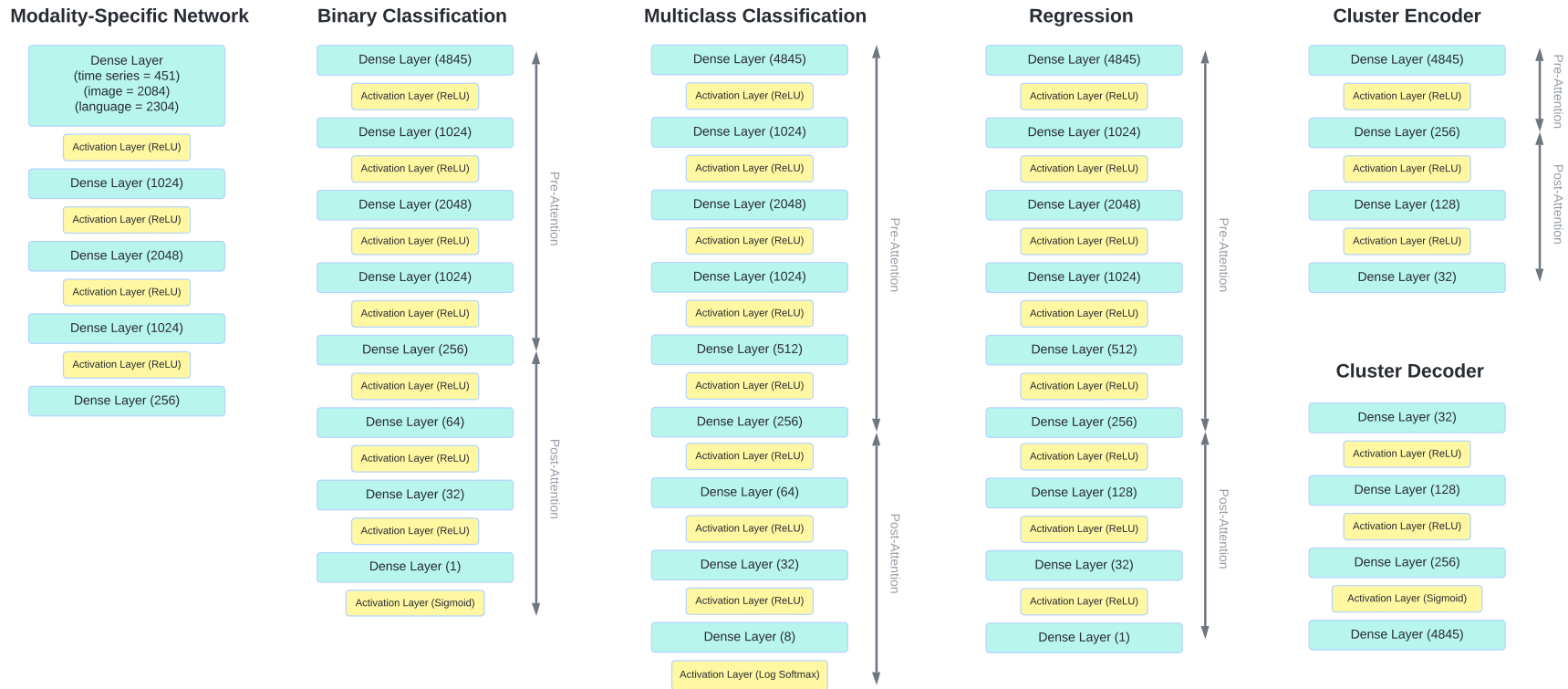
Healthcare Task	Disease Grouping	Disease Names	Identification Criterion
Disease Diagnosis	Blood Disorder	Anemia	By diagnosis name
	Cardiovascular Medicine	Heart Failure	By diagnosis name
		Ischemic Heart Disease	By diagnosis name
	Critical Care	Sepsis	By diagnosis name
		Stroke	By diagnosis name
	Endocrinology	Obesity	By diagnosis name
		Osteoporosis	By diagnosis name
		Diabetes	By diagnosis name
	Gastroenterology and Hepatology	Chronic Liver Disease	By diagnosis name
		Inflammatory Bowel Disease	<i>ICD 10</i> K50 – K52 <i>ICD 9</i> 555
	Infectious Diseases	Antimicrobial Resistance	By diagnosis name
		Bacterial Intestinal Infections	<i>ICD 10</i> A00 – A09 <i>ICD 9</i> 001 – 009
		Hepatitis B/C	By diagnosis name

Disease Diagnosis	Infectious Diseases	HIV/AIDS	By diagnosis name
		Tuberculosis	By diagnosis name
	Internal Medicine	Fibromyalgia	By diagnosis name
	Nephrology	Chronic Kidney Disease	By diagnosis name
	Neurology	Alzheimer's Disease	By diagnosis name
		Epilepsy	By diagnosis name
		Parkinson's Disease	By diagnosis name
	Oncology	Breast Cancer	<i>ICD 10</i> C50 <i>ICD 9</i> 1570 – 1574 1578 – 1579
		Leukemia	By diagnosis name
		Lymphoma	By diagnosis name
		Melanoma	By diagnosis name
		Prostate Cancer	<i>ICD 10</i> C61 <i>ICD 9</i> 185
	Ophthalmology	Glaucoma	By diagnosis name
		Macular Degeneration	By diagnosis name
	Psychiatry and Psychology	Bipolar Disorder	By diagnosis name

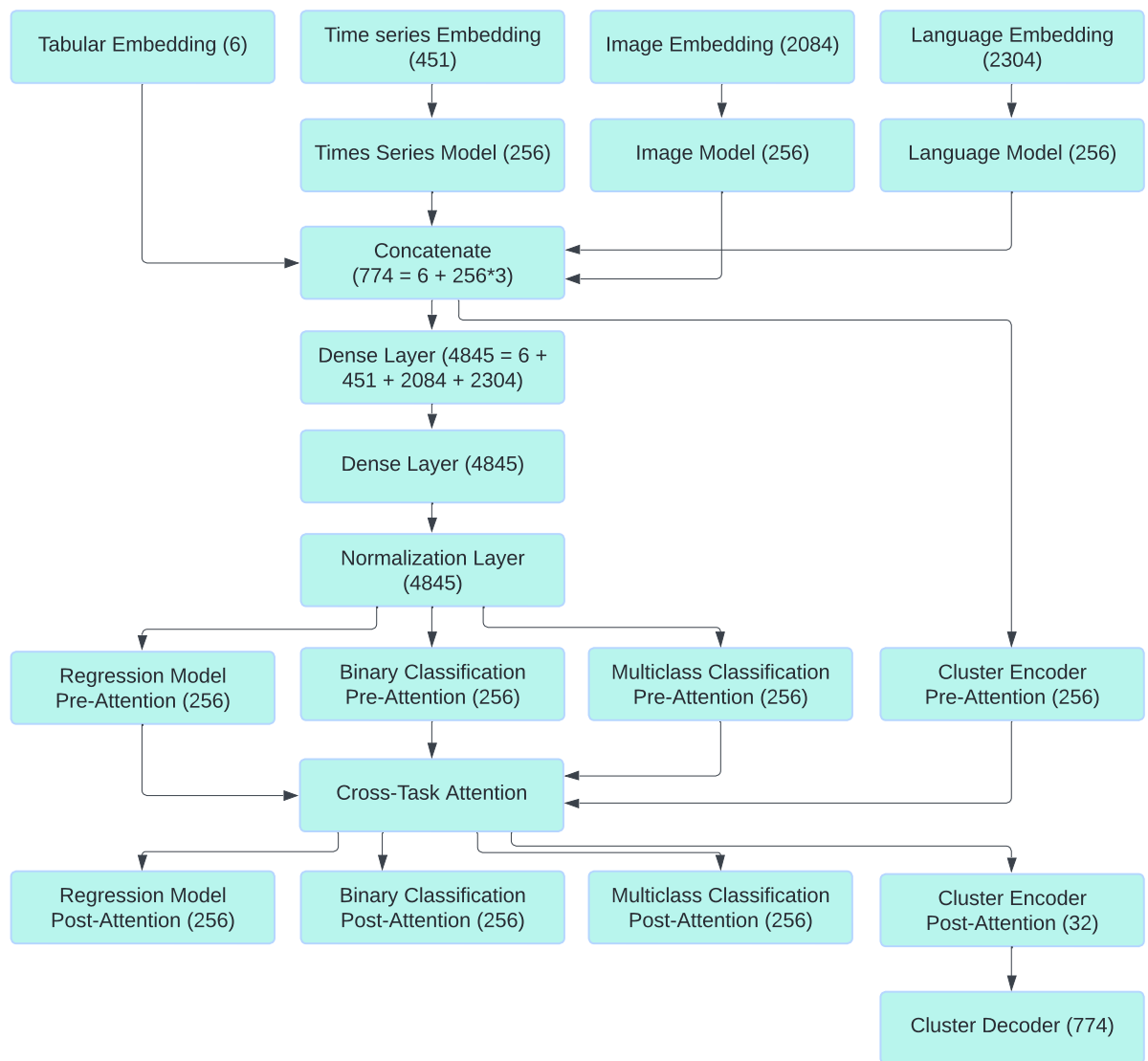
Disease Diagnosis	Psychiatry and Psychology	Major Depressive Disorder	By diagnosis name
		Schizophrenia	By diagnosis name
	Pulmonary diseases	Asthma	By diagnosis name
		Chronic Obstructive Pulmonary Disease	By diagnosis name
		Pneumonia	By diagnosis name
	Rheumatology	Gout	By diagnosis name
		Lupus	By diagnosis name
	Urology	Urinary Incontinence	By diagnosis name
	Thoracic Testing	Atelectasis, cardiomegaly, consolidation, edema, enlarged cardio mediastinum (enlarged CM), lung opacity, pneumonia, pneumothorax	By ground truth from data
	General Mortality	Mortality in the next 48 hours	By discharge status and discharge time
Hospital Operations	Length of Stay	Number of days left in hospital	By discharge time
	Hospital Acquired Infection	Catheter-related-bloodstream infection	<i>ICD 10</i> A41.01 A41.02 B95.61 B95.62 T80.2- T82.7-
			<i>ICD 9</i> 038.11 038.12 041.11 041.12 996.62 999.3x
		Nosocomial pneumonia	<i>ICD 10</i>

			A48.1 B01.2 B05.2 J10.0- J11.0- J12-J18 <i>ICD 9</i> 480x 481 482x 483x 485 486 487.0 997.3x
Hospital Operations	Hospital Acquired Infection	Surgical site infection	<i>ICD 10</i> J10.0- J11.0- J12- J13 J14 J15 J16- J17 J18- O86.0- T81.4 T81.8- T84.5 – T84.7 T88.0- T88.8- Z48.8- <i>ICD 9</i> 483x 485 486 587.0 569.61 682x 996.6x 997.3x 996.7x 998.5x 998.6 999.34 999.39
		Urinary tract infection	<i>ICD 10</i> N10 N15- N16 N30- N30.81 N39.0 N99.89 T83.5- <i>ICD 9</i> 590.1x 590.2 590.8x 590.9 595.0 596.4 599.0 996.64 997.5
Patient Phenotyping	Patient Subgroup	Patient subgroup	None, all data included

Supplemental Table 1. Identification criterion for each healthcare task.



Supplemental Figure 2. Architecture details of each modality-specific and task-specific network.



Supplemental Figure 3. Overall Pipeline of the M3H Architecture.

Algorithm 1 Cross-Task Attention for MultiTask Learning

Input:

s : Set of tasks to be jointly learned
 N : Number of batches
 α : Exploration strength parameter for cross-task learning
 $x_s^i \in \mathbb{R}^{n_{\text{batch}} \times n_{\text{tasks}} \times n_{\text{feature}}}$: Task embedding tensor from batch i
 $T_s \in \mathbb{R}^{1 \times n_{\text{tasks}}}$: Task tokens tensor of form $[0, 1, 2, \dots, n_{\text{tasks}} - 1]$
 $I_s \in \mathbb{R}^{n_{\text{batch}} \times n_{\text{tasks}} \times n_{\text{tasks}}}$: Identity tensor to encourage self learning

Output:

$O_s \in \mathbb{R}^{n_{\text{batch}} \times n_{\text{tasks}} \times n_{\text{feature}}}$: Cross-learned embedding output.

Initialize Linear Transformations: Initialize linear transformations for queries, keys, and values: $W_Q, W_K, W_V \in \mathbb{R}^{n_{\text{feature}} \times n_{\text{feature}}}$, and task token linear transformation $W_T \in \mathbb{R}^{n_{\text{feature}} \times n_{\text{tasks}}}$.

```
for  $i \leq N$  do
     $Q_s \leftarrow W_T \cdot T_s$             $\triangleright$  Convert task tokens vector  $T_s$  into task embeddings
     $Q_s \leftarrow W_Q \cdot Q_s$           $\triangleright$  Compute query vectors from task embeddings
     $K_s \leftarrow W_K \cdot x_s$           $\triangleright$  Compute key vectors from task embeddings
     $V_s \leftarrow W_V \cdot x_s$           $\triangleright$  Compute value vectors from task embeddings
     $M_s \leftarrow Q_s \cdot K_s^\top$        $\triangleright$  Compute Attention Weight
     $W_s \leftarrow \text{softmax} \left( I_s + \frac{\alpha M_s}{\max(M_s)} \right)$   $\triangleright$  Normalize by maximum weight entry,
    scale by exploration strength, and encourage self-learning
     $O_s \leftarrow W_s \cdot V_s$             $\triangleright$  Output the cross-learned embeddings
end for
```

Supplemental Figure 4. Algorithmic representation of cross-task attention learning.